Future Energy
Open Access Journal
ISSN 2832-0328

May 2024| Volume 03 | Issue 02 | Pages 01-15

Journal homepage: https://fupubco.com/fuen

https://doi.org/10.55670/fpll.fuen.3.2.1

Future Publishing LLC

Article

Comparative analysis of electrochemical behaviors of lithium-ion batteries using the dual potential MSMD battery models: case studies on various thermal conditions

Nirjhor Barua, Md. Arafat Rahman*, Md. Mamunur Roshid

Department of Mechanical Engineering, Chittagong University of Engineering and Technology, Chittagong-4349, Bangladesh

ARTICLE INFO

Article history:
Received 12 May 2023
Received in revised form
25 June 2023
Accepted 15 July 2023

Keywords:
Electrochemical, Simulation, Lithium-Ion Battery, Multi-Scale-Multi-Domain Model, Thermal Conditions

*Corresponding author
Email address:
arafat@cuet.ac.bd

DOI: 10.55670/fpll.fuen.3.2.1

ABSTRACT

The high energy density and long cycle life of lithium-ion batteries make them a preferred option for electric vehicles. The efficiency and life span of lithium-ion batteries are particularly sensitive to temperature; thus, it becomes essential to maintain an ideal temperature range. In this context, we concentrated on two widely used electro-chemistry (Equivalent Circuit Model and NTGK) models of a single cell of a dual potential MSMD Lithium-ion Battery while taking into account two significant methods of heat transfer under varying C-rates (0.25C, 1C, 2C, and 5C). We investigated the highest temperatures that two e-chemistry models could reach in varying ambient temperatures (typical summer, winter, and room temperature). The maximum temperature-raising tendency in the ECM due to natural convection is greater than the maximum temperature-raising tendency due to radiation regardless of the environmental temperatures and various C rates (0.25C, 1C, and 2C). However, the trend line of the maximum temperature rise is different in the NTGK model, where the maximum temperature rise due to radiation is greater than the maximum temperature rise due to convection for 0.25C, 1C, and 2C rates in -5°C and 40°C environmental temperatures. In the NTGK model, at 0.25C, 1C, and 2C rates for winter and summer temperatures, the maximum temperature rise owing to radiation is larger than that due to convection. The NTGK model, however, produced somewhat superior findings for the radiation mode of heat transfer at ambient temperature. Therefore, it can be said that convection is a better thermal condition than natural convection in the NTGK model.

1. Introduction

Consumers are familiar with lithium-ion batteries after a great deal of research and use. It is commonly used in electrical items and electric cars. In recent years, a potential market for electric urban vehicles has formed, with competitive series among mobile device manufacturers. A special focus is being paid to developments in high-performance lithium-ion batteries (such as a high level of energy density, high open circuit voltage, and minimal self-discharge). Despite the widespread use of lithium-ion batteries in portable and small electronic devices, there are still some important issues that need to be resolved before practical applications of electrical vehicles (EVs), hybrid electrical vehicles (HEVs), and microgrids with significant energy storage capacity can be taken into account. Heat control and management are the most critical concerns in lithium-ion batteries, as excessive temperatures reduce charge/discharge efficiency and battery life and can potentially pose a safety risk. The significant temperature increase that occurs during the charging and discharging of HEVs and EVs is the main cause for worry in the heat regulation of lithium-ion batteries (LIBs) since it may result in thermal runaway. Understanding lithium-ion battery discharge behavior is crucial for the thermal management of LIBs in hybrid electric vehicles and electric vehicles [1]. Although a lot of research work has been conducted in recent years to enhance the thermal management of Li-ion batteries; however, relatively few have been devoted to the

investigation of the discharge behavior of lithium-ion batteries using ANSYS FLUENT. In common parlance, there is a relationship between battery temperature variation and electric efficiency. However, to make battery modeling simpler, it is frequently done by using a one-dimensional mass transfer model, which may work at least for cells with parallel plate electrodes. Chen and Evans suggested that due to the anisotropic thermal characteristics of a stack of many cells, a two -or three-dimensional model (of heat transmission) is required for battery thermal modeling and established a mathematical model to analyze the thermo-physical properties of LIBs and LPBs (lithium polymer batteries) [2]. The purpose of thermal management was to analyze how factors in battery design and working conditions affect the temperature rise and profile and to assess the risk of thermal lag. The modeling results showed that under typical battery operation, battery temperatures were unlikely to reach the temperature that triggers thermal runaway, while during high-rate discharge (for example, during the relatively brief period of intense power extraction from a battery), heat may not be transferred out of a large cell stack. Localized heating may raise battery temperature to the thermal runaway onset temperature within one minute, according to research on heat transfer in the presence of extremely focused heat sources caused by battery abuse (such as short circuits). A Battery modeling at a constant environmental temperature of 25°C only, which was based on the localized heat production approach, considering a manganese oxide spinel/carbon cell using a 2D-coupled thermal-electrochemical technique, has been reported [3, 4]. The matrix and solution phases of the model include reversible, irreversible, and Ohmic heat. Most of the research works focused only on the convection mode of heat transfer for a better thermal management system of a Lithium-ion battery [5-7]. Van et al. [8] analyzed the effects of forced convection in the thermal management system. However, very few studies were carried out concerning radiation as the primary thermal condition. Hatchard et al. suggested that Radiation may be responsible for up to 50% of the heat that a Li-ion cell releases into the environment at oven exposure conditions. The label is usually the outermost surface of the cell, and its emissivity determines how well heat is transferred by radiation [9]. In this present study, we focused on two commonly used electro-chemistry (ECM and NTGK) models of a single cell of a dual potential MSMD Lithium-ion Battery considering two dominant methods of heat transfer under various C-rates. We compared the maximum temperatures achieved by two e-chemistry models under different environmental temperatures (winter, room temperature, and summer). We compared the simulation results to explore which e-chemistry model performs better in thermal management systems under various environmental temperatures.

2. Model development

In this study, ANSYS FLUENT (Version 2023 Ansys-R1) software was used to perform the computational fluid dynamic (CFD) analysis, which makes use of the finite-volume approach to separate the physics equations by figuring out the mathematical equations of the fluids. The combined heat transmission nodal points, which include two dominant heat transfer methods, including convection and radiation, are modeled using mathematical formulas. ANSYS commonly uses the following models to predict the behavior of chemical, thermal, and electrical processes in a battery:

- Empirical Battery Model with Single Potential
- Multi-Scale Multi-Domain Dual-Potential Battery Model (MSMD)

2.1 Single-potential empirical battery model

This model is based on investigations that have been performed by [10] and [11]. The integral form of the electric potential equation is as follows:

$$\int_v \nabla.(\sigma\nabla\phi)\,dV = \int_A j dA \quad (1)$$

The term "A" stands for apparent current density, "j" for local interface area, and "ϭ" for electrical conductivity. For the Single Potential Empirical Battery Model (SPEBM) The mathematical equations are used according to [10] and [11]:

$$j = Y(\phi_c - \phi_\alpha - U) \quad (2)$$

Here, $(\phi_c - \phi_\alpha)$ is the Difference between the cathode and anode side electric potentials at the separator interface, and Y and U are GU's parameters. The single-potential empirical battery model (SPEBM) is limited in its capacity to study a wide range of electrochemical events in battery systems, especially those with complex geometries.

2.2 Multi-scale multi-domain (MSMD) dual-potential battery model

By effectively linking the physics of batteries, battery discharge, safety, and thermal management, the multi-scale multi-domain (MSMD) battery model, sometimes referred to as the "multi-scale multi-domain" battery model, is used to study the discharge of lithium-ion batteries. The ANSYS FLUENT Dual Potential Multiscale Multi-Dimensional Battery Model (MSMD) addresses various physics in many solution domains by using a homogenous model related to a multiscale multidimensional method to resolve these constraints. It is important to note that the MSMD method uses three different electrochemical submodels, which are as follows:

- The Newman, Tiedemann, Gu, and Kim (NTGK) model.
- Equivalent Circuit Model (ECM).
- Newman's Pseudo-2D (Newman's P2D) model.

In this study, Equivalent Circuit Model (ECM) and The Newman, Tiedemann, Gu, and Kim (NTGK) models are discussed considering various C-rates, States of Charge, and Depth Of Charge. The ECM model, which works with batteries of all types, not only Li-ion batteries, is both affordable and highly adaptable. Using a 2D table that plots each parameter against the temperature and SOC. Notably, this is the only form where the impact of temperature is taken into account explicitly. In charge/discharge cycles when the electric load doesn't exhibit any sudden fluctuations, the NTGK model is satisfactory. Additionally, some models, such as the ECM, will be more accurate if the electric load changes quickly since they neglect the inertial variations. However, the pseudo-2D model, created by Newman's team utilizing a porous electrode and concentrated solution theory, is a physics-based model that accurately simulates the transit of lithium ions in a battery [12]. Although Newman's pseudo-2D model is the most popular electrochemistry model, it is computationally more expensive than the other two e-

chemistry models [12]. So, for computational simplicity, only ECM and NTGK models are discussed in this study.
The multiscale multidomain (MSMD) technique is useful for assessing various physical parameters in several solution domains. Based on the conservation of charge during discharge, the Poisson equations are as follows:

$$\nabla.(\sigma+\nabla\phi+)|_{\Omega+} = -j \quad (3)$$

$$\nabla.(\sigma-\nabla\phi-)|_{\Omega-} = +j \quad (4)$$

Here, the effective electrical conductivities of the positive and negative electrodes are σ^+ and σ^-, the phase potentials of the positive and negative electrodes are ϕ^+ and ϕ^-, the transfer rate of the volumetric current, calculated using an electrochemical submodel, is j (A/m^3), and the domains of the positive and negative electrodes are Ω^+ and Ω^-, respectively. The functional form is determined by the electrode polarisation curve. H. Gu and Huo et al. found that j varies linearly with cell voltage [11] and [13]. The NTGK model was suggested by Kwon et al. [14]:

$$j = \alpha Y[U - (\phi+ - \phi-)] \quad (5)$$

where, α is the specific area m^2/m^3 of the electrode sandwich sheet in the battery cell, while U and Y are the empirical fitting parameters. The following U and Y functions were proposed by Huo et al. [13].

$$U = a_o + a_1(DOD) + a_2(DOD)^2 + a_3(DOD)^3 + a_4(DOD)^4 + a_5(DOD)^5 \quad (6)$$

$$Y = b_o + b_1(DOD) + b_2(DOD)^2 + b_3(DOD)^3 + b_4(DOD)^4 + b_5(DOD)^5 \quad (7)$$

Where, the coefficients a_i and b_i (i = 0, . . . 5) are constants to be calculated experimentally. The fitting parameters used to determine the potential and current density distributions on the electrodes during discharge are shown in Table 1.

Table 1. The fitting parameters were used in the NTGK model

Parameter	Constant	Value
U	a0	4.3104
	a1	-1.9184
	a2	2.8835
	a3	-6.8305
	a4	-9.7601
	a5	-4.8786
Y	b0	879.2
	b1	-4606.2
	b2	-23,007.5
	b3	-86,540.6
	b4	101,993.2
	b5	-44,914.4

According to Van-Thanh et al. [8], the nominal capacity multiplied by the C rate equaled the discharging current, and the discharge rate dictated how long a battery could operate. The lower the discharge rate, the longer the battery could operate. The maximum temperature was outside the manufacturer's working range at discharge conditions greater than 3C. Yi et al. [15] discovered that the ambient temperature is extremely sensitive during this sort of experiment. Because of the electron transfer during electrochemical processes, a substantial amount of heat is created in the Li-ion battery at a high discharge rate. The Li-ion battery's heat generation q (W) is separated into three parts: reaction heat q_r (W) polarisation heat q_p (W), and Joule heat q_j (W) [13]. The volumetric heat source in the battery cell can be expressed as irreversible heat from the internal resistance of the cell j[Voc - (ϕ+ - ϕ-)] and reversible heat from the electrochemical reaction inside the cell $-jT\frac{dVoc}{dT}$. Moreover, the heat produced by the resistance of the current collecting tab and the electrical contact between it and the lead wire is included, however, the heat produced by the resistance of the electrical contact between it and the lead wire is excluded. The entire amount of heat generated can be expressed as the equation given by Van-Thanh et al. [8]:

$$q = j[V_{oc^-}(\phi+ - \phi-) - T\frac{dVoc}{dT}] + \sigma + V^2\phi + \sigma - V^2\phi^- \quad (8)$$

where, V_{oc} is the open-circuit potential of the cell (V), and T is the working temperature of the battery.
We have considered two different dominant thermal conditions (convection and radiation) to study the cases of different discharge rates. According to Newton's law of cooling, the quantity of heat dissipated owing to the movement of a fluid (air) can be calculated using the following equation.

$$q_a = h_a(T_b - T_a) \quad (9)$$

where T_b is the battery temperature, T_a is the ambient temperature and h_a is the coefficient of air convective heat transfer coefficient of air, which is 5 W/m^2k in this present study.
In this study, we illustrated the effect of radiation heat transfer in the thermal management system for both electrochemistry models (NTGK and ECM). Hence, we have considered the radiation emissivity of the battery cell to the maximum possible (ε = 1). The heat dissipation of a single cell of a Lithium-Ion Battery can be calculated by the equations used by Hatchard et al. [9].

$$P_r(T) = A\sigma\varepsilon(T^4 - T_w^4) \quad (10)$$

where $P_r(T)$ is radiation power in J/s as a function of temperature, A is the surface area, T_w is the temperature of the surrounding (assumed to be a black body), and ε is the emissivity of the surface. Emissivity (ε) is a dimensionless quantity between 0 and 1. It represents the fraction of blackbody radiation that the surface in question emits (a black body by definition has ε = 1), σ is the Stefan-Boltzmann constant (5.669 x 10-12 W/(cm^2 K)). For values of T near T_w, Eq (10) can be expanded in a Taylor series:

$$P(T) = 4A\sigma\varepsilon T_W^3\Delta T + 6A\sigma\varepsilon T_W^2\Delta T^2 + 4A\sigma\varepsilon T_W\Delta T^3 + A\sigma\varepsilon\Delta \quad (11)$$

Here, ΔT is the temperature difference between the surface and the surroundings and if $\Delta T = T_w - T$, rearranging Eq (11) gives

$$\frac{P(T)}{A\Delta T} = 4\sigma\varepsilon T_w^3 + 6\sigma\varepsilon T_w^2\Delta T + 4\sigma\varepsilon T_w\Delta T^2 + \sigma\varepsilon\Delta T^3 \quad (12)$$

Eliakim and Karmeli put out an accurate, acceptable, and comprehensive electrical battery model [16]. Figure 1 shows the electrical battery model that was used in the equivalent

circuit model. The six-parameter ECM model has been adopted by ANSYS [1].

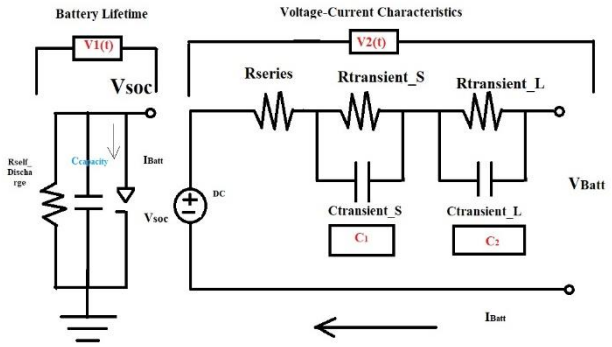

Figure 1. The electrical battery model is used in the ECM model [1]

Where, Rseries=Rs, Rtransient_ S=RI, Rtransient_ L=R2. The voltage-current relationship can be obtained by solving the following mathematical formulas of electrical circuits used by Madani et al. [1] and M. Chen et al. [16]:

$$V(t) = V_{OCV}(SOC) + V_1 + V_2 + R_2(SOC)I(t) \quad (13)$$

$$\frac{dV_1}{dt} = -\frac{1}{R_1(soc)C_1(soc)}V_1 - \frac{1}{C_1(soc)}I(t) \quad (14)$$

$$\frac{dV_2}{dt} = -\frac{1}{R_2(soc)C_2(soc)}V_2 - \frac{1}{C_2(soc)}I(t) \quad (15)$$

$$\frac{d(soc)}{dt} = -\frac{I(t)}{3600Q_{Ah}} \quad (16)$$

The open-circuit voltage, resistor resistances, and capacitor capacitances are dependent on the state of charge of the battery for a specific battery (SOC). These two dependents can be illustrated in various procedures in ANSYS as the following set of equations used by [1] and [16]:

$$R_s = a_o + a_1(SOC) + a_2(SOC)^2 + a_3(SOC)^3 + a_4(SOC)^4 + a_5(SOC)^5 \quad (17)$$

$$R_1 = b_o + b_1(SOC) + b_2(SOC)^2 + b_3(SOC)^3 + b_4(SOC)^4 + b_5(SOC)^5 \quad (18)$$

$$C_1 = c_o + c_1(SOC) + c_2(SOC)^2 + c_3(SOC)^3 + c_4(SOC)^4 + c_5(SOC)^5 \quad (19)$$

$$R_2 = d_o + d_1(SOC) + d_2(SOC)^2 + d_3(SOC)^3 + d_4(SOC)^4 + d_5(SOC)^5 \quad (20)$$

$$C_2 = e_o + e_1(SOC) + e_2(SOC)^2 + e_3(SOC)^3 + e_4(SOC)^4 + e_5(SOC)^5 \quad (21)$$

$$VOC_s = f_o + f_1(SOC) + f_2(SOC)^2 + f_3(SOC)^3 + f_4(SOC)^4 + f_5(SOC)^5 \quad (22)$$

Chen's function is represented by the following set of equations [16] :

$$R_s = a_0\exp[a_1(soc)] + a_2 \quad (23)$$

$$R_1 = b_0\exp[b_1(soc)] + b_2 \quad (24)$$

$$C_1 = c_0\exp[c_1(soc)] + c_2 \quad (25)$$

$$R_2 = d_0\exp[d_1(soc)] + d_2 \quad (26)$$

$$C_2 = e_0\exp[e_1(soc)] + e_2 \quad (27)$$

$$V_{ocv} = f_0\exp[f_1(soc)] + f_2 \quad (28)$$

The source terms for the aforementioned equations are calculated as the following [1] :

$$j_{ECh} = I/Vol \quad (29)$$

$$\dot{q_{ECh}} = \frac{I}{Vol}\left[V_{ocv} - (\phi^+ - \phi^-) - T\frac{dU}{dT}\right] \quad (30)$$

Where, Vol=The battery volume, I= Current, Vocv= The open circuit voltage, and ϕ^+& $\phi^-$are phase potentials.

2.2.1 Physical modeling

A single Lithium-Ion Battery cell has been modeled using ANSYS DESIGN MODULER. A three-dimensional rectangular-shaped battery cell is designed.

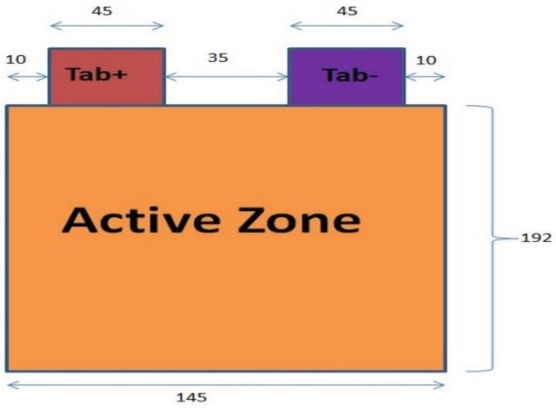

Figure 2. Dimensions of a single-cell Li-ion battery

In Figure 2, the geometry and dimensions of the single cell of the MSMD dual potential Lithium-Ion battery are illustrated. All the units are taken as millimeters. The thickness of the cell is taken as 2mm. The Geometry properties of the simulation are given in Table 2.

Table 2. Geometrical properties of the experiment

Details of Body	
Body	FFF/Solid
Volume	5.568e-05 m^3
Surface Area	0.057028 m^2
Faces	6
Edges	12
Verticles	8
Fluid/Solid	Solid
Shared Topology Method	Automatic
Geometry Type	Workbench

2.2.2 Mesh generation

To assure the accuracy of transient simulations, grid number is crucial. Mesh details of the experiment are given in Table 3.

2.2.3 Material selection

There are mainly two types of material defined in the MSMD battery model. They are fluid and solid materials. The Fluid material is defined as 'AIR' and The solid material is defined with three different materials. The active cell zone is

defined as lithium hexafluorophosphate. The positive electrode is defined as aluminum and the negative electrode is defined as copper. The Material properties are provided in Tables 4-7.

Table 3. Details of the mesh of the experiment

Element order	Linear
Element size	1.e-003m
Growth rate	default by ANSYS (1.2)
Average surface area	3.6582e-003 m^3
Maximum Layers	5
Inflation Algorithm	Pre-Executive
Mesh metric	Skewness
Nodes	97230
Elements	63780

Table 4. Active cell zone material properties (lithium hexafluorophosphate)

Material name	Lithium hexafluorophosphate
Density	1500 kg/m^3
Specific Heat Coefficient	871 j/(kg K)
Electrical conductivity	1e+07 S/m

Table 5. Positive electrode material properties (Aluminium)

Material name	Aluminium
Density	2092 kg/m^3
Specific Heat Coefficient	871 j/(kg k)
Electrical conductivity	3.541e+07 S/m

Table 6. Negative electrode material properties (Copper)

Material name	Copper
Density	8978 kg/m^3
Specific Heat Coefficient	381 j/(kg k)
Electrical conductivity	1e+07 S/m

Table 7. Surrounding fluid properties (Air)

Material name	Air
Density	1.225 kg/m^3
Specific Heat Coefficient	1006.43 j/(kg k)
Electrical conductivity	defined per UDS S/m
Viscosity	1.7894e-05

3. Results and discussion

To analyze the results two dominant thermal conditions (Convection, and radiation) have been considered, and the two most common electrochemical models (ECM and NTGK) are used. We have varied the C rates(0.25C, 1C, 2C, and 5C) to analyze the thermal conditions of a single cell of the MSMD dual potential Lithium-ion battery. In the case of convection, certain boundary conditions are also taken into account. The temperature of the free stream temperature (-5°C, 27°C, and 40°C) is varied considering different temperature conditions according to the average temperature of the winter and summer seasons of Bangladesh. The heat transfer coefficient is taken as 5 W/m^2k for each case of the free stream temperature. The initial heat generation rate is considered to be 0 W/m^3. For radiation, we have considered the same temperatures for external radiation (-5°C, 27°C, and 40°C). We have considered the entire outer surface of the single cell of the Lithium-ion battery as a black body and therefore took the maximum emissivity of the surface (ε=1). The same thermal conditions are implemented in both ECM and NTGK models, and then we carried out our simulations for 1000 iterations and 1500 seconds flow time. The lowest stop voltage and the highest stop voltage are considered as 3v and 4.3v respectively, and the nominal capacity of the battery cell is considered as 14.6 Ah.

3.1 Equivalent circuit model

3.1.1 Thermal condition: convection

Typically, heat generation within the LIBs occurs at normal temperatures as a result of charge transfer and chemical processes during charging and discharging [17, 18]. The total heat generation of battery discharge consists mainly of electrochemical reaction heat, ohmic heat, and active polarization heat. During the battery's discharge, these temperatures are generated in the positive electrode, electrolyte, and negative electrode. The three types of heat-generating sources mentioned above vary in cell space. Lithium extraction and intercalation occur during the discharge electrochemical process at the anode/electrolyte and cathode/electrolyte interfaces, respectively. Lithium extraction heat and lithium intercalation heat are two different components of the electrochemical process heat. Similarly to this, the terms for lithium extraction and intercalation make up the active polarization heat. The anode and cathode electron-conduction resistance as well as the ion-conduction resistance contribute to the ohmic heat [17]. To understand the thermal behavior and overall heat generation resulting from the aforementioned sources, we explored the ECM e-chemistry model based on different boundary conditions (Convection and Radiation) considering different environmental temperatures. Contours of total static temperatures in the whole cell of the dual potential MSMD Li-Ion Battery are shown in Figure 3, Figure 4, and Figure 5 considering the boundary conditions as convection for various environmental temperatures of 268K, 300K, and 313K respectively. The nominal capacity multiplied by the C rate gave the discharging current its value. The discharge rate of a battery determines its working time, so the greater the discharge rate, the longer the battery's operating period will be.

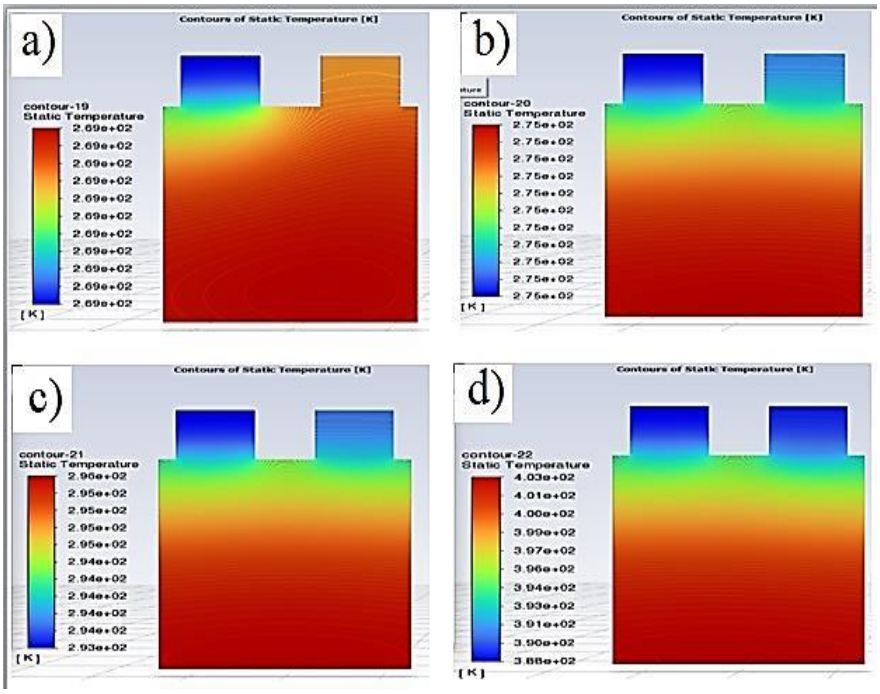

Figure 3. Temperature variation in a single cell of dual potential MSMD Li-Ion Battery with various C-rates with Equivalent Circuit Model considering free stream temperature of 268k: a) for 0.25C-rate, b) for 1C-rate, c) for 2C-rate, and d) for 5- rate

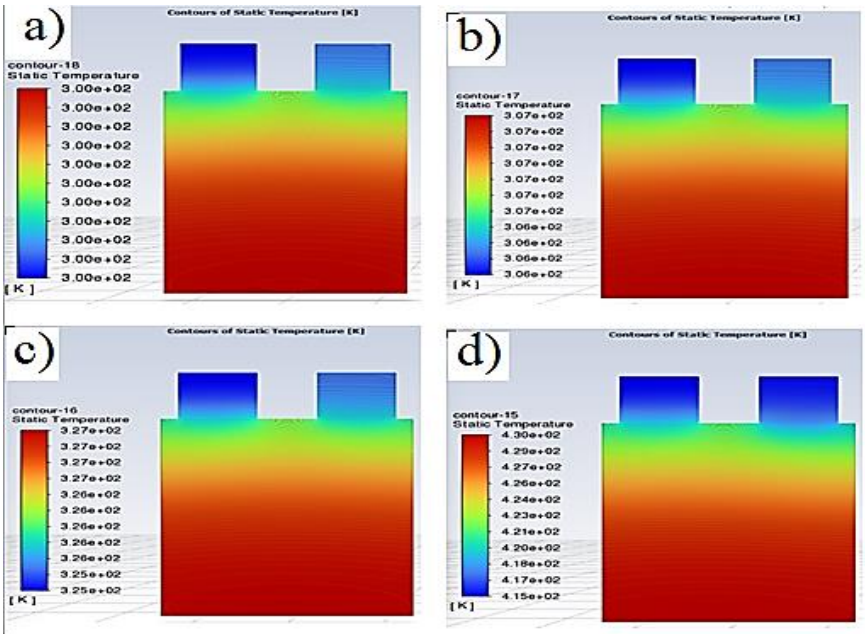

Figure 4. Temperature variation in a single cell of a dual-potential MSMD Li-Ion battery with various C rates with an equivalent circuit model considering free stream temperature of 300k: a) for 0.25C-rate, b) for the 1C rate, c) for the 2C rate and d) for the 5- rate

In Figure 3, temperature variations are shown in a single cell of dual potential MSMD Li-Ion Battery with various C-rates (0.25C, 1C, 2C, and 5C) with Equivalent Circuit Model. Natural convection is considered in the boundary condition. The free stream temperature is taken as 268K (typical winter temperature in Asia). In Figure 3(a), for the 0.25 C rate, the minimum temperature is 268.6371 K, and the maximum temperature is 268.6637 K, which shows a very slight increase from the environmental temperature (268K). In Figures 3(b), 3(c), and 3(d), the C-rate was varied from 1 C, 2 C, and 5 C, and the maximum temperature was obtained 275.0931 K, 295.6211 K, and 402.9109 K respectively. As we can see for increased C-rates, the maximum temperatures are increased rapidly. For 1 C, the maximum temperature increased by only 2.64%, while for the 2 C rate the battery cell showed a significant temperature rise of 10.30% from the

ambient temperature, and for the 5 C rate, the temperature rose drastically by 50.339% from the ambient temperature. The simulation ended after 570s for 5 C-rate because the maximum temperature at the 5 C rate was above the designated operating range.

In Figure 4, temperature variations are shown in a single cell of dual potential MSMD Li-Ion Battery with various C-rates(0.25C, 1C, 2C, and 5C) with Equivalent Circuit Model considering natural convection as the boundary condition, and the free stream temperature is taken as 300K (room temperature in Asia). Just like in Figure 3, the temperature variations show a similar pattern in Figure 4. In Figures 4(a), 4(b), 4(c), and 4(d), the maximum temperatures for 0.25C, 1C, 2C, and 5C rates are 300.4373 K, 306.8669 K, 327.3949 K, and 430.1342 K respectively. For 0.25 C, the maximum temperature is slightly increased, while for 1C, 2C, and 5C rates the maximum temperature rose to 2.28%, 9.13%, and 43.37% from the ambient temperature.

In Figure 5, temperature variations are shown in a single cell of dual potential MSMD Li-Ion Battery with various C-rates(0.25C, 1C, 2C, and 5C) with Equivalent Circuit Model considering natural convection as the boundary condition, and the free stream temperature is taken as 313K (typical summer temperature in Asia). Just like in Figure 3 and Figure 4, the temperature variations show a similar pattern in Figure 5. In Figures 5(a), 5(b), 5(c), and 5(d), the maximum temperatures for the 0.25C, 1C, 2C, and 5C rates are 313.3455K, 319.775K, 340.303K, 441.1937 K, respectively. For 0.25 C, the maximum temperature is just slightly increased from the environmental temperature, while for 1C, 2C, and 5C rates the maximum temperature rose 2.258%, 8.723%, and 40.96% respectively from the ambient temperature.

In Figures (3-5), it is seen that for higher environmental temperatures the maximum temperature increase rate is lowered in each C-rates for convective boundary conditions. This is because the ambient temperature has significant effects on the electrolyte property in the Li-ion battery [19]. However, the maximum temperatures for each C rate tend to rise higher with an increase in environmental temperatures. In each case, the maximum temperature is obtained in the active cell zone regardless of the C-rates and environmental temperature.

3.1.2 Thermal condition: radiation

The configuration of the cell's surface has a significant impact on how much heat is released by radiation. The label is usually the cell's exterior surface, and its emissivity determines how well heat is transferred via radiation. Li-Ion Battery Cells with the largest thermal endurance will result from choosing labels with the highest possible emissivity (ε = 1) [9]. Therefore, in this study, we have considered the maximum possible external thermal emissivity (ε = 1) for each case. We have considered the initial heat generation rate to be 0 W/m^3. Contours of total static temperatures in the whole cell of the dual potential MSMD Li-Ion battery are shown in Figure 3, Figure 4, and Figure 5 considering the boundary conditions as radiation for various external radiation temperatures of 268K, 300K, and 313K, respectively.

In Figure 6, temperature variations are shown in a single cell of dual potential MSMD Li-Ion Battery with various C-rates (0.25C, 1C, 2C, and 5C) with Equivalent Circuit Model. Radiation is considered in the boundary condition.

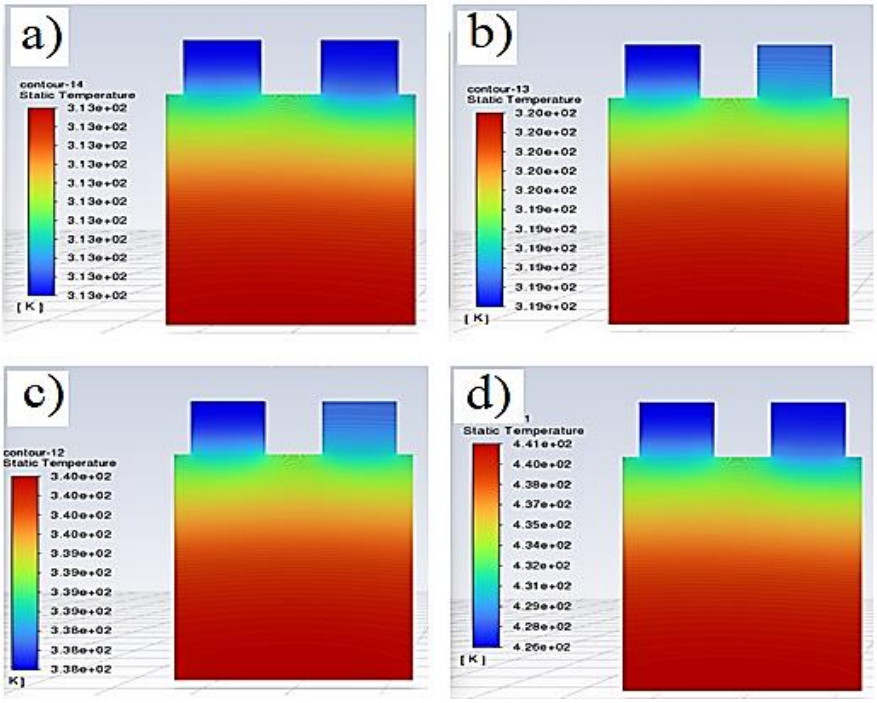

Figure 5. Temperature variation in a single cell of dual potential MSMD Li-Ion Battery with various C-rates with Equivalent Circuit Model considering free stream temperature of 313k: a) for 0.25C-rate, b) for 1C-rate, c) for 2C-rate and d) for 5- rate

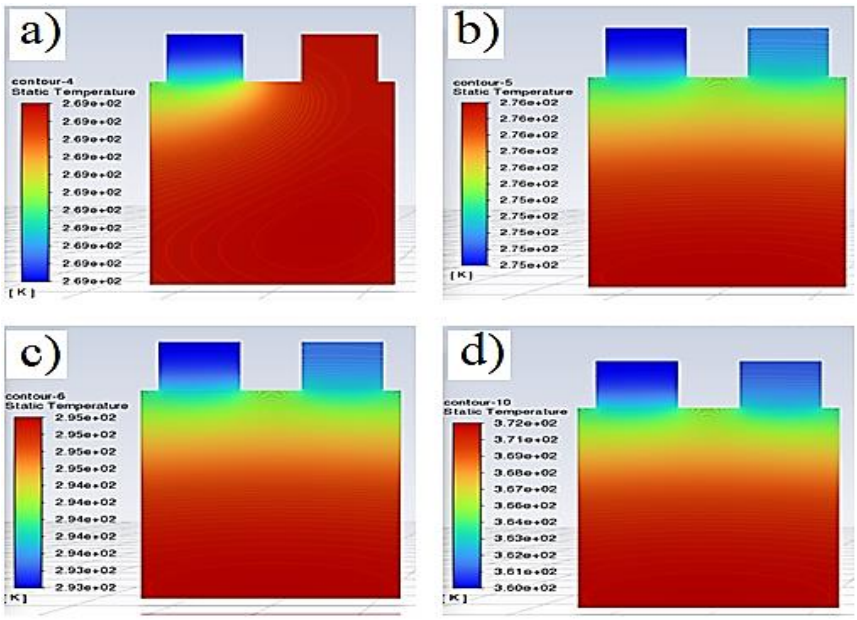

Figure 6. Temperature variation in a single cell of dual potential MSMD Li-Ion Battery with various C-rates with Equivalent Circuit Model considering external radiation temperature of temperature of 268K: a) for 0.25C-rate, b) for 1C-rate, c) for 2C-rate and d) for 5- rate

The external radiation temperature is taken as 268 K (typical winter temperature in Asia). In Figure 6(a), for 0.25 C rate and maximum temperature is 268.8422K. which shows a very slight increase from the environmental temperature(268K). In Figures 6(b), 6(c), and 6(d), the C-rate was varied from 1 C, 2 C, and 5 C, and the maximum temperature was obtained 275.7793K, 295.33K, and 371.8228K respectively. For the 1C rate, then the maximum temperature of the single Li-Ion battery cell increased up to 2.90% from the environmental temperature. The maximum temperature considerably rose with greater C rates. For the 2 C rate, the maximum temperature rose by 10.19% and for the 5C rate, the maximum temperature increased rapidly to 38.73% from the ambient temperature. While taking the heat transfer mode as radiation, the maximum temperature exceeded the designated working range for 5 C, and the simulation stop conditions arrived after 570s just like the previously discussed convective boundary conditions.

In Figure 7, temperature variations are shown in a single cell of a dual potential MSMD Li-Ion battery with various C rates (0.25C, 1C, 2C, and 5C) with the Equivalent Circuit Model considering radiation as the heat transfer mode. The external radiation temperature is taken as 300 K (room temperature in typical Asia). Figure 7(a) shows that the maximum temperature obtained for the 0.25 C rate is 300.3606 K, which is almost the same as the environmental temperature. From Figures 7(b), 7(c), and 7(d) we can see that for higher C-rates higher temperatures are obtained. For 1C, 2C, and 5C the maximum temperatures are found as 305.5259K, 320.6266K, and 386.0818K respectively. At 1C rate, the maximum temperature increased by only 1.84%. For higher C rates, the maximum temperature rose rapidly. For 2C and 5C rates, the maximum temperature increased up to 6.87% and 28.69% from the ambient temperature, respectively.

In Figure 8, temperature variations are shown in a single cell of a dual-potential MSMD Li-Ion battery with various C-rates (0.25C, 1C, 2C, and 5C) with an Equivalent Circuit Model considering Radiation as heat transfer mode. The external radiation temperature is taken as 313 K (typical summer temperature in Asia). Figure 8(a) shows that the maximum temperature obtained for the 0.25 C rate is 313.0591K, which is almost the same as the environmental temperature. From Figures 8(b), 8(c), and 8(d) we can see that, for 1C, 2C, and 3C the maximum temperature is 314.2582K, 317.8055K, and 419.8545K. It indicates that for 1C, 2C, and 5C the maximum temperature increased by up to 0.40%, 1.535%, and 34.13% from the ambient temperature, respectively.

In the aforementioned Figures 6-8, increasing the environmental temperatures, the maximum temperature increase rate is decreased in each C-rates for radiative boundary conditions, which shows a similar trend discussed in Figures 3-5. However, the maximum temperatures for each C rate tend to rise higher with an increase in environmental temperatures. In each case, the maximum temperature is obtained in the active cell zone regardless of the C-rates and environmental temperatures.

3.2 NTGK model

3.2.1 Thermal condition: convection

To comprehend the physics underlying the complicated nature of lithium-ion batteries, electrothermal models are crucial. In this study, we focus on two commonly used electronic chemistry models to analyze the results comparatively. In Figures 9, 10, and 11, we discussed the maximum temperatures obtained by the single cell of an MSMD dual potential Li-Ion Battery considering the boundary conditions as natural convection. We varied the environmental temperature (free stream temperature) to explore the thermal behavior of Li-ion batteries in different situations.

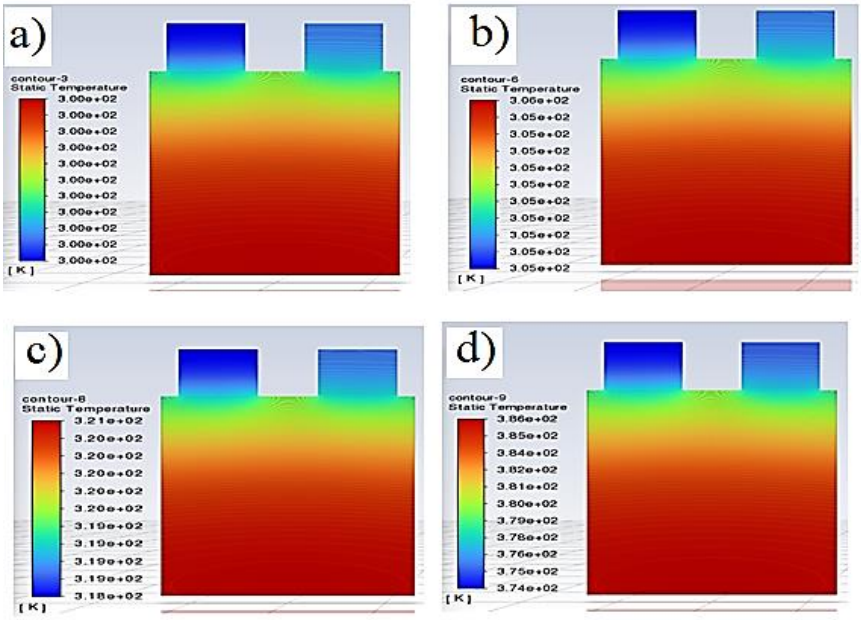

Figure 7. Variation of temperature in a single cell of a dual-potential MSMD Li-Ion battery with various C rates with an equivalent circuit model considering an external radiation temperature of 300 K: a) for 0.25C-rate, b) for the 1C rate, c) for the 2C rate and d) for the 5- rate

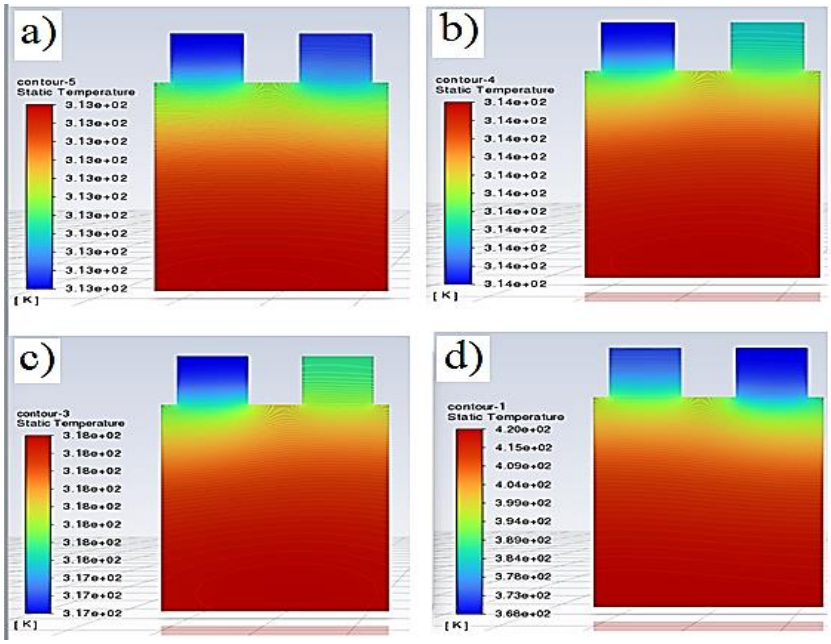

Figure 8. Variation in temperature in a single cell of dual potential MSMD Li-Ion battery with various C-rates with Equivalent Circuit Model considering the external radiation temperature of 313 K: a) for 0.25C-rate, b) for the 1C rate, c) for the 2C rate and d) for the 5- rate

Contours of total static temperatures in the whole cell of the dual potential MSMD Li-Ion Battery are shown in Figure 9, Figure 10, and Figure 11 considering the boundary conditions as Convection for various environmental temperatures of 268K, 300K, and 313K, respectively. The nominal capacity multiplied by the C rate gave the discharging current its value, just as same as in the previously discussed ECM e-chemistry model. The discharge rate of a battery determines its working time, so the greater the discharge rate, the longer the battery's operating period will be [6].

In Figure 9, temperature variation in a single cell of a dual potential MSMD Li-Ion battery is shown with the NTGK electrochemistry model for various C rates while the boundary conditions are taken as natural convection. The environmental temperature is considered 268 K (typical winter temperature in Asia). Figures 9(a), 9(b), 9(c) and 9(d) represent the temperature variations in the battery cell for 0.25C, 1C, 2C, and 5C rates, respectively. It is seen that for the 0.25C rate, the maximum temperature increased to 268.4804K, which is slightly higher than the ambient

temperature. For 1C, 2C, and 5C rates, the maximum temperatures were 272.3053 K, 281.8218 K, and 439.7356 K, respectively. For 1C, the maximum temperature increased only 1.60% from the environmental temperature, while for higher C rates, it increased rapidly. For 2C and 5C rates, the maximum temperatures increased up to 5.15% and 64.08% respectively. It shows that, in the NTGK model, the maximum temperature increase rate rapidly increases with higher C rates. For the 5 C rate, the battery simulation stop condition arrived after 570 s.

In Figure 10, temperature variations are shown in a single cell of the dual-potential MSMD Li-Ion battery with various C-rates(0.25C, 1C, 2C, and 5C) with the NTGK model considering natural convection as the boundary condition and the temperature of the free stream is taken as 300K (room temperature in Asia). In Figure 10(a), it is shown that the maximum temperature increased by 300.1283K, which is almost the same as the environmental temperature.

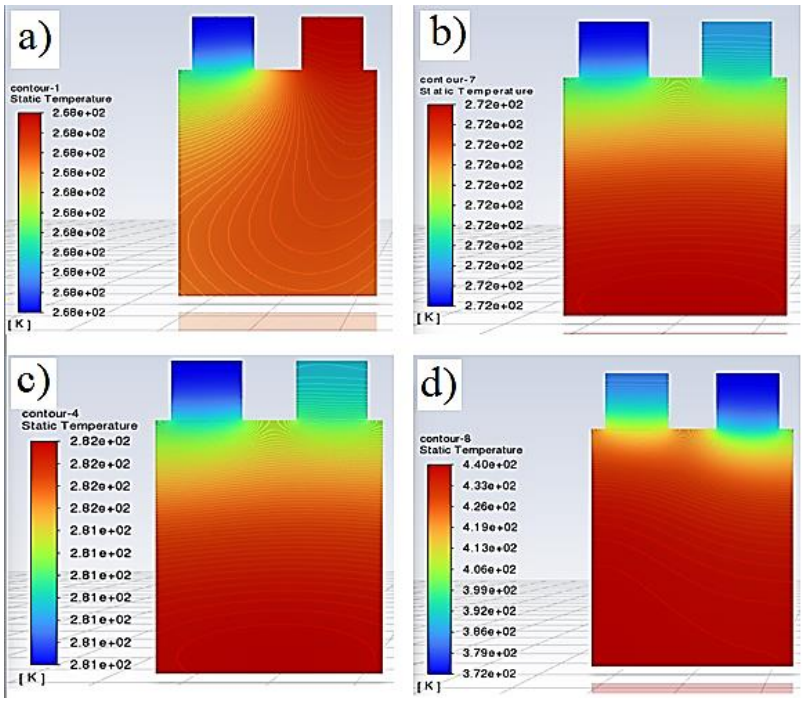

Figure 9. Variation in temperature in a single cell of a dual potential MSMD Li-Ion battery with various C rates with the NTGK model considering the free flow temperature of 268 K: a) for 0.25C-rate, b) for the 1C rate, c) for the 2C rate, and d) for the 5- rate

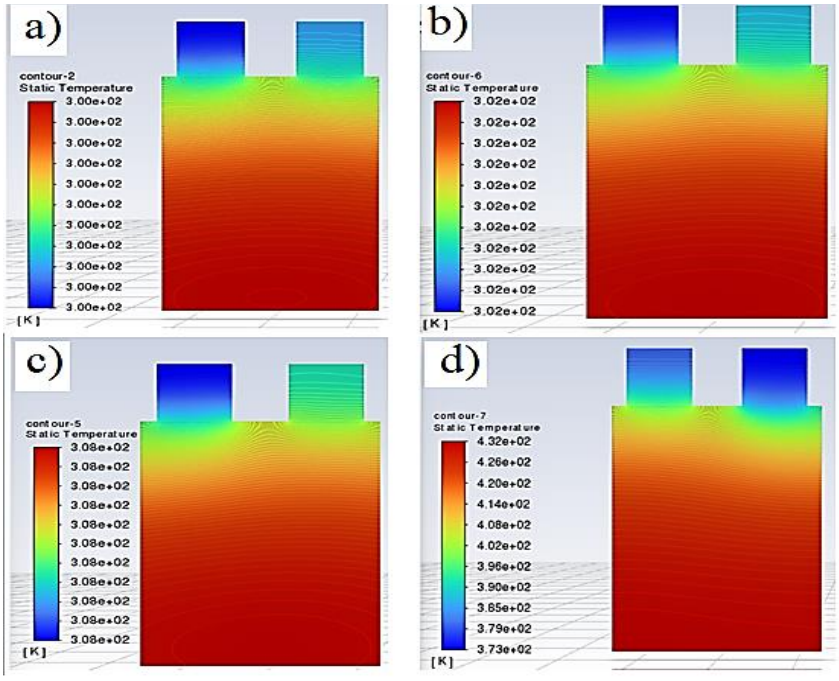

Figure 10. Variation of temperature in a single cell of a dual-potential MSMD Li-Ion battery with various C rates with the NTGK model considering the free stream temperature of 300 K: a) for 0.25C-rate, b) for the 1C rate, c) for the 2C rate, and d) for the 5-rate

From Figures 10 (b), 10 (c), and 10(d) we see that the maximum temperatures obtained for 1C, 2C, and 5C were 302.19K, 308.111K, and 431.601K respectively. For 1C, 2C, and 5C rates the maximum temperatures increased up to 0.73%, 2.70%, and 43.86% respectively from the environmental temperatures.

In Figure 11, temperature variations are shown in a single cell of dual potential MSMD Li-Ion Battery with various C-rates (0.25C, 1C, 2C, and 5C) with NTGK Model considering natural convection as the boundary condition, and the free stream temperature is taken as 313K (typical summer temperature in Asia). The temperature variations show a similar pattern in Figure 11 just like in Figures 9 and 10. In Figures 11(a), 11(b), 11(c), and 11(d), the maximum temperatures for 0.25C, 1C, 2C, and 5C rates are 313.0101 K, 314.6604 K, 319.5787 K, and 429.6515 K respectively. For 0.25 C, the maximum temperature is just slightly increased from the environmental temperature, while for 1C, 2C, and 5C rates the maximum temperature rose 0.53%, 2.101%, and 37.26% respectively from the ambient temperature. Figure 11 also showed a similar trend to the previous analysis where the maximum temperature increase rate decreased with the increase of the environmental temperatures. However, the maximum temperature always increased with the increase of C rates.

3.2.2 Thermal condition: radiation

We considered the maximum possible external thermal emissivity (ε = 1) for each case in the NTGK model, just like the model of the equivalent circuit previously discussed. We considered the initial heat generation rate to be 0 W/m^3. Figures 12, 13, and 14 depict contours of total static temperatures across the dual potential MSMD Li-Ion Battery's whole cell where boundary conditions are regarded as radiation for varying external radiation temperatures of 268K, 300K, and 313K, respectively.

In Figure 12, temperature variations are shown in a single cell of dual potential MSMD Li-Ion Battery with various C-rates (0.25C, 1C, 2C, and 5C) with NTGK Model. Radiation is considered in the boundary condition. The external radiation temperature is taken as 268 K (typical winter temperature in Asia). In Figure 12(a), the 0.25 C rate and the maximum temperature are 268.8422K which shows a very slight increase from the environmental temperature (268K). In Figures 12 (b), 12 (c), and 12(d), the C-rate was varied from 1 C, 2 C, and 5 C, and the maximum temperature was obtained 275.7793 K, 295.33 K, and 371.8228 K, respectively. For the 1C rate, the maximum temperature of the single Li-Ion battery cell increased up to 2.90% from the environmental temperature. For higher C rates, the maximum temperature increased significantly. For the 2 C rate, the maximum temperature rose by 10.19% and for the 5C rate, the maximum temperature increased rapidly to 38.73% from the ambient temperature. While taking the heat transfer mode as radiation, at 5 C rate the maximum temperature was outside the specified operating range, and the simulation stop conditions arrived after 570s just like the previously discussed convective boundary conditions. In Figure 13, the external radiation temperature is taken as 300K (room temperature in typical Asia), and temperature variations in a single cell of MSMD dual potential Li-ion battery are shown. In Figure 13(a), the maximum temperature for the 0.25C rate is 300.1069K, which is only slightly higher than the environmental temperature. The maximum temperature increased rapidly with higher C rates. In the aforementioned Figures 13(b), 13(c), and 13(d) for 1C, 2C, and 5C the maximum temperature obtained was 301.8011K, 306.5999K, and 421.5734 K, respectively. For 1C, 2C, and 5C the maximum temperature increased to 0.60%, 2.199%, and 40.52% respectively.

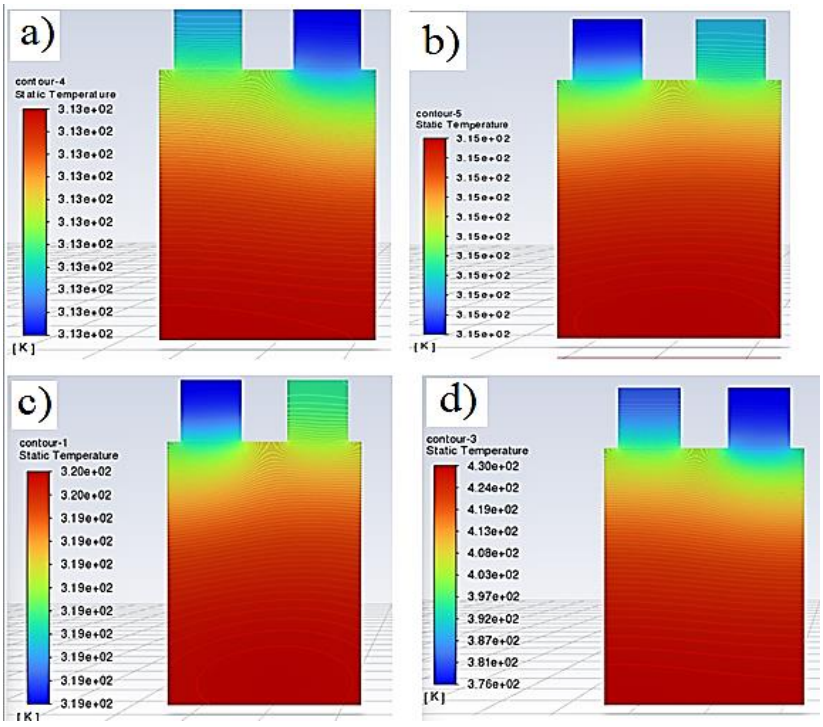

Figure 11. Variation in temperature in a single cell of dual potential MSMD Li-Ion battery with various C-rates with the NTGK model considering the free-flow temperature of 313k: a) for 0.25C-rate, b) for 1C rate, c) for 2C rate and d) for 5- rate

For the 5C rate at room temperature, the temperature in the battery cell increased drastically which indicates the battery conditions were outside the specified operating range. As the battery geometry was quite low and comparatively a large amount of current discharging conditions was provided, the battery simulation stop condition arrived and indicated a thermal runaway. In Figure 14, the external radiation temperature is taken as 313K (typical summer temperature in Asia), and temperature variations in a single cell of MSMD dual potential Li-ion battery are shown.

In the aforementioned Figure 14 (a), the maximum temperature for the 0.25C rate is 313.3035K, which is only slightly higher than the environmental temperature. For higher C rates, the maximum temperature increased rapidly. In the aforementioned figures 14 (b), 14 (c), and 14(d) for 1C, 2C, and 5C the maximum temperature obtained was 317.8952K, 331.4985 K, and 392.7853K respectively. For 1C, 2C, and 5C the maximum temperature increased by up to 1.56%, 5.9%, and 25.49% respectively.

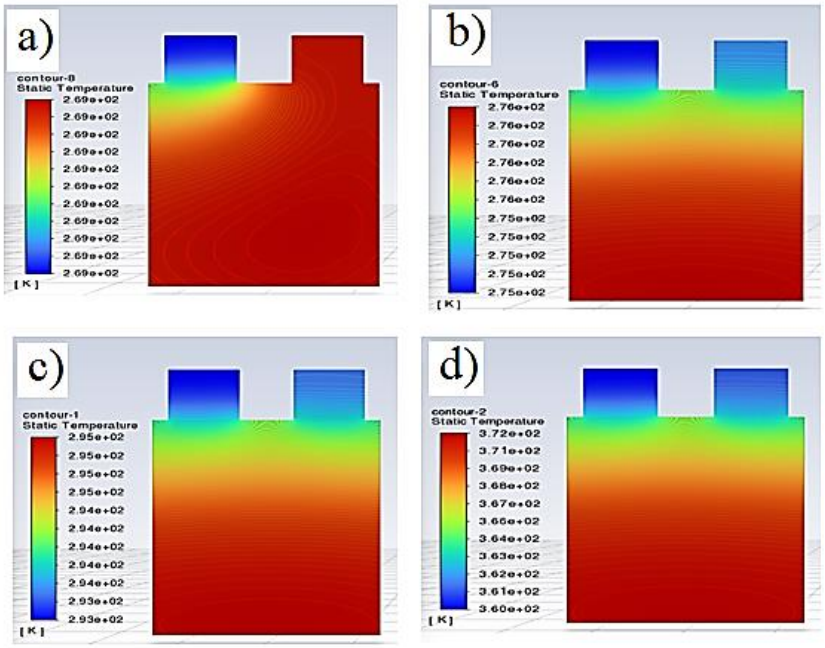

Figure 12. Variation in temperature in a single cell of dual potential MSMD Li-Ion battery with various C-rates with the NTGK model considering an external radiation temperature of 268 K: a) for 0.25C-rate, b) for 1C rate, c) for 2C rate and d) for 5- rate

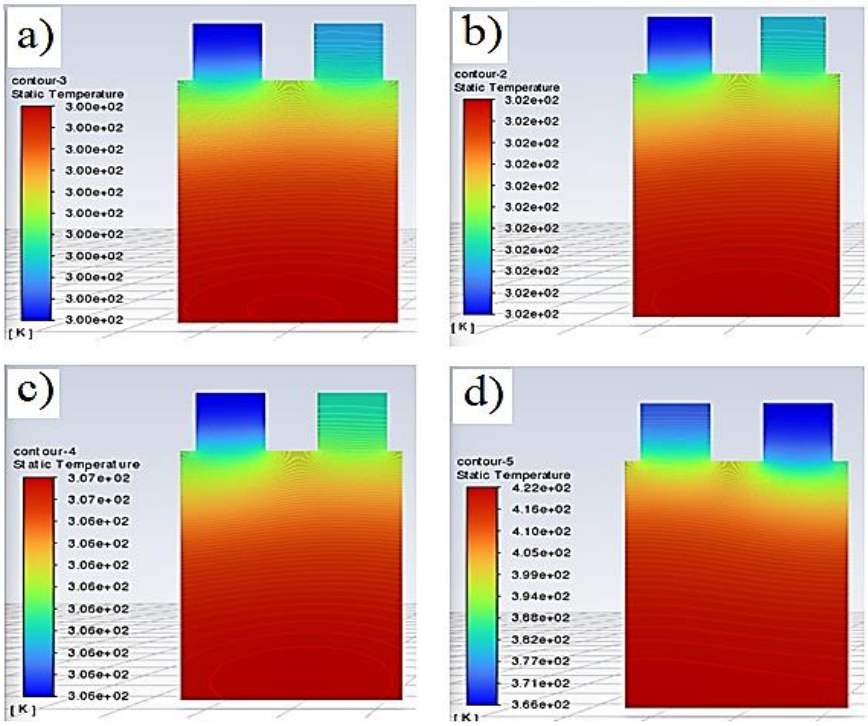

Figure 13. Variation of temperature in a single cell of a dual-potential MSMD Li-Ion battery with various C rates with the NTGK model considering an external radiation temperature of 300 K: a) for 0.25C-rate, b) for the 1C rate, c) for the 2C rate, and d) for the 5-rate

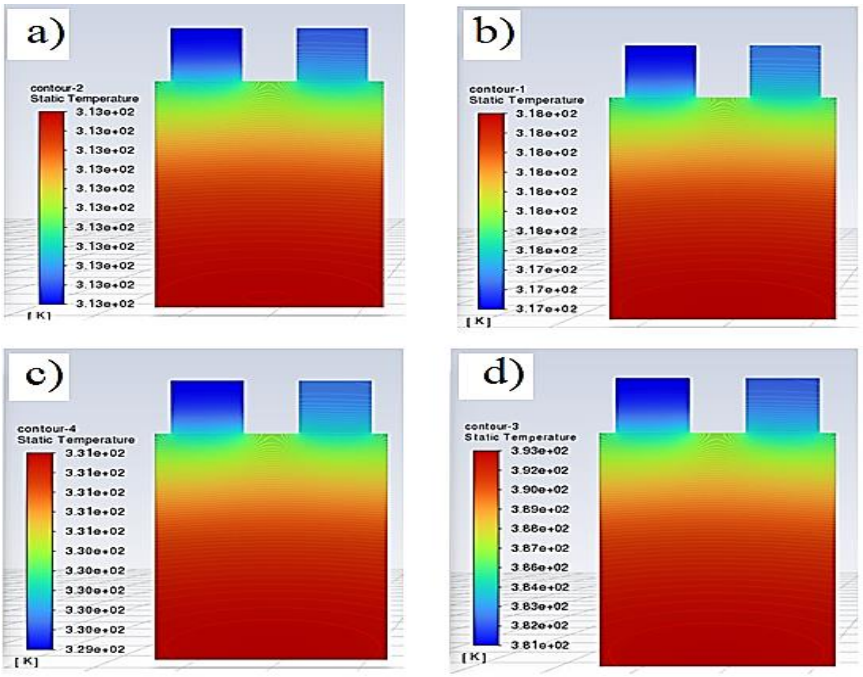

Figure 14. Variation of temperature in a single cell of a dual-potential MSMD Li-Ion battery with various C rates with the NTGK model considering an external radiation temperature of 313 K: a) for 0.25C-rate, b) for the 1C rate, c) for the 2C rate, and d) for the 5-rate

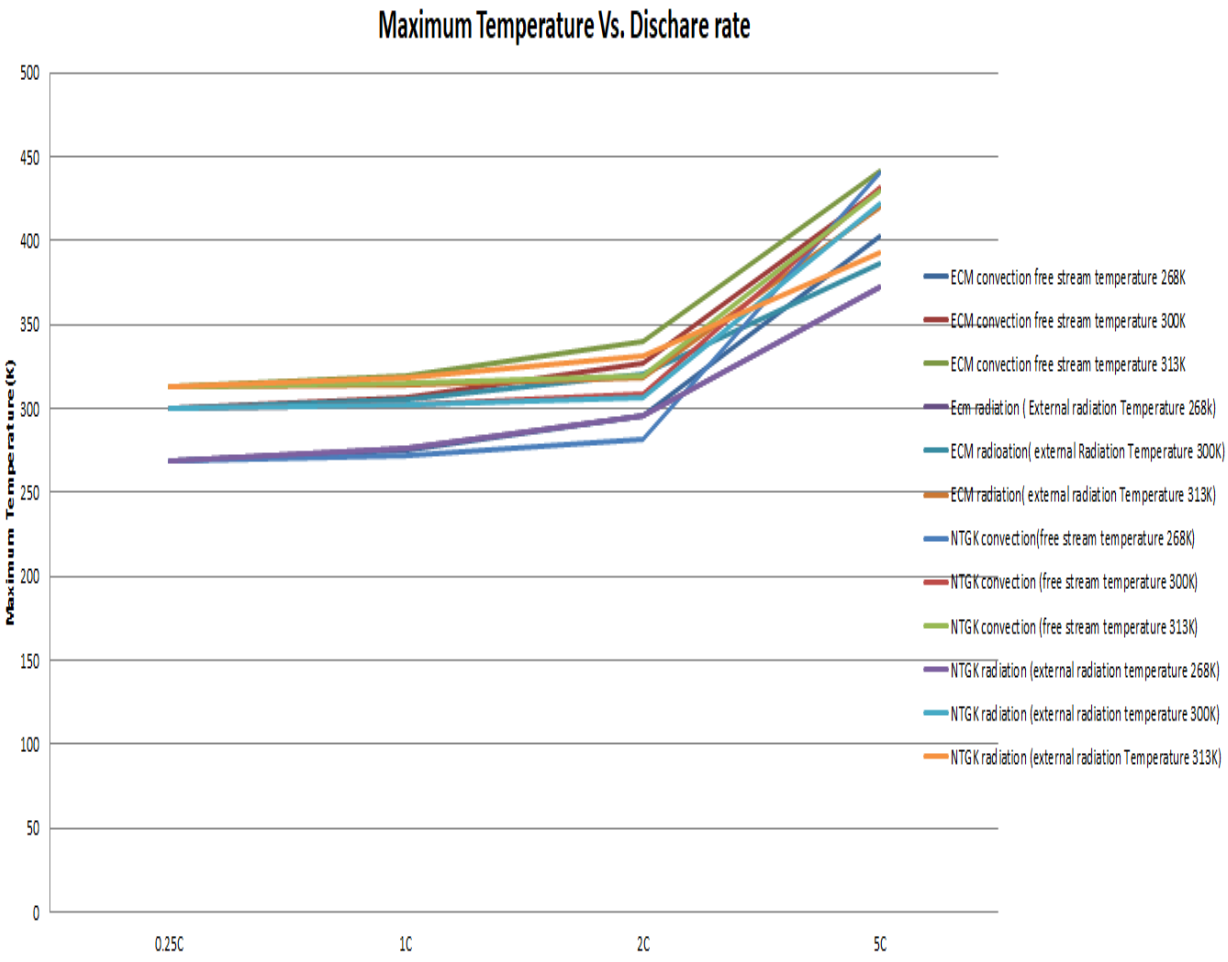

Figure 15. Maximum temperature vs. discharge rate for the ECM and NTGK models with different thermal conditions

From Figures 12, 13, and 14, it is observed that, for higher environmental temperatures, the increase rate of the maximum temperature from the environmental temperature is comparatively lower in the NTGK model than in the ECM model, while the boundary conditions are considered as radiation. Just like the previously discussed convective boundary conditions for the NTGK e-chemistry model in Figures (6-8), Figure 12, Figure 13, and Figure 14 also showed a similar trend where the maximum temperature increased with increasing environmental temperature. The maximum temperature was always obtained in the Active Material (electrolyte) zone.

In Figure 15, the maximum temperature vs. discharge rate is shown for both ECM and NTGK e-chemistry models considering convective and radiative boundary conditions. In each case, it is observed that for higher Discharge rates the maximum temperatures increased rapidly. Up to 2 C rate, the battery was inside the specified operating conditions and the temperature increased stably. However, at a high C rate (5 C), in each case, the battery was beyond operational condition. Due to the specified maximum and minimum stop voltages of the battery, the materials property of the battery cell, and the geometry of the battery cell, a sharp increase was observed in each environmental condition at 5C, regardless of the boundary conditions. The environmental temperature had a significant effect on the increase rate of the maximum temperatures. It was because the environmental temperature played a crucial role in the activation energy inside the Li-ion battery cell.

4. Conclusion

We have seen for each of the electrochemical models, the temperature rises drastically after the 2C rate and the maximum stop condition of the simulation arrived just after 570s. For the ECM model while taking the thermal condition as natural convection and the free stream temperature as 268K, 300K, and 313K respectively, the highest temperature of the MSMD dual potential Lithium-ion Battery the single cell raised to 402.9109K, 430.1342K, and 441.1937K respectively for 5C discharge rate. For the ECM model, in the natural convection mode of heat transfer, the battery cell temperature increased by up to 9.48% while the environmental temperature changed from winter (-5°C) to summer (40°C) temperature. For radiation, The battery cell temperature is increased to 371.8288 K, 386.0818 K, and 419.8545 K for 5C rate with the corresponding environmental radiation temperature 268 K, 300 k, 313 k, which means the temperature increase rate of the cell raised to 12.91% but the maximum temperatures are lower than the ECM model's highest temperatures for convection in each case. From Figure 13 it is also clearly visible that for various discharge rates (0.25C, 1C, and 2C), the maximum temperature-raising tendency in the ECM due to natural convection is greater than the maximum temperature-raising tendency due to radiation regardless of the environmental temperature (-5°C, 27°C, and 40°C). Therefore, radiation is found to be a better thermal condition than natural convection in the ECM model. However, the trend line of the maximum temperature rise is opposite in the NTGK model, where the maximum temperature rise due to radiation is greater than the maximum temperature rise due to convection for 0.25C, 1C, and 2C rates at -5°C and 40°C environmental temperatures. For 5C in the NTGK model, the magnitude of maximum temperatures showed a variation from the temperature-raising trend line in Figure.13 which was due to the arrival of the maximum stop condition of the simulation, where the simulation stopped just after 570 s of flow time. In the NTGK model, the maximum temperature rise due to radiation is greater than that due to convection for 0.25C, 1C, and 2C rates for winter and summer temperatures. However, at room temperature, the radiation mode of heat transfer showed a bit better result in the NTGK model. So, it can be said that in the NTGK model, convection is a better thermal condition than natural convection. After analyzing the simulation results of the highest temperatures reached by implementing two different electrochemical models in a single cell of a dual potential MSMD Lithium-Ion battery, we can conclude that the radiative thermal condition of the e-chemistry of the equivalent circuit model is just a little better than the convective thermal condition of the NTGK model at elevated summer temperature (40°C). However, the convective thermal condition of the NTGK model shows a significantly better thermal management system and less heat generation in winter (-5°C) and at room temperature(27°C) compared to the radiative thermal condition of the ECM model.

Acknowledgment

This work is supported by the University Grants Commission of Bangladesh-grant no. 37.01. 0000.73.06.065.22.1607. The corresponding author is responsible for ensuring that the descriptions are accurate and agreed upon by all authors.

Ethical issue

The authors are aware of and comply with best practices in publication ethics, specifically concerning authorship (avoidance of guest authorship), dual submission, manipulation of figures, competing interests, and compliance with policies on research ethics. The authors adhere to publication requirements that the submitted work is original and has not been published elsewhere in any language.

Data availability statement

Data sharing does not apply to this article as no datasets were generated or analyzed during the current study.

Conflict of interest

The authors declare no potential conflict of interest.

References

[1] S. S. Madani, M. J. Swierczynski, and S. K. Kaer, "The discharge behavior of lithium-ion batteries using the Dual-Potential Multi-Scale Multi-Dimensional (MSMD) Battery Model," 2017 12th Int. Conf. Ecol. Veh. Renew. Energies, EVER 2017, 2017, doi: 10.1109/EVER.2017.7935915.

[2] Y. Chen and J. W. Evans, "Thermal Analysis of Lithium-Ion Batteries," vol. 143, no. 9, pp. 2708–2712, 1996.

[3] V. Srinivasan and C. Y. Wang, "Analysis of Electrochemical and Thermal Behavior of Li-Ion Cells," J. Electrochem. Soc., vol. 150, no. 1, pp. A98–A106, 2003, doi: 10.1149/1.1526512.

[4] W. B. Gu and C. Y. Wang, "Thermal-Electrochemical Modeling of Battery Systems," J. Electrochem. Soc., vol. 147, no. 8, p. 2910, 2000, doi: 10.1149/1.1393625.

[5] K. Smith and C. Y. Wang, "Power and thermal characterization of a lithium-ion battery pack for hybrid-electric vehicles," J. Power Sources, vol. 160, no. 1, pp. 662–673, 2006, doi: 10.1016/j.jpowsour.2006.01.038.

[6] C. At, “Transient Thermal Analysis of a Fin,” pp. 1–16, 2020.
[7] J. Duan et al., “Modeling and analysis of heat dissipation for liquid cooling lithium-ion batteries,” Energies, vol. 14, no. 14, 2021, doi: 10.3390/en14144187.
[8] K. Van-Thanh, Ho; Khoungsik, Chang; Sang Wook, Lee; Sung Han, “Transient Thermal Analysis of a Li-Ion Battery,” 2020.
[9] T. D. Hatchard, D. D. MacNeil, D. A. Stevens, L. Christensen, and J. R. Dahn, “Importance of heat transfer by radiation in Li-ion batteries during thermal abuse,” Electrochem. Solid-State Lett., vol. 3, no. 7, pp. 305–308, 2000, doi: 10.1149/1.1391131.
[10] Haariet Martique, “This is a reproduction of a library book that was digitized by Google as part of an ongoing effort to preserve the information in books and make it universally accessible. https://books.google.com,” Oxford Univ., vol. XXX, p. 60, 1994.
[11] H. Gu, “Mathematical Analysis of a Zn / NiOOH Cell,” J. Electrochem. Soc., vol. 130, no. 7, pp. 1459–1464, 1983, doi: 10.1149/1.2120009.
[12] C. Vanaclocha Hervas, “Comparative study of three electrochemical cell models for the CFD simulation of a battery module,” 2021.
[13] Y. Huo, Z. Rao, X. Liu, and J. Zhao, “Investigation of power battery thermal management by using mini-channel cold plate,” Energy Convers. Manag., vol. 89, pp. 387–395, 2015, doi: 10.1016/j.enconman.2014.10.015.
[14] K. H. Kwon, C. B. Shin, T. H. Kang, and C. S. Kim, “A two-dimensional modeling of a lithium-polymer battery,” J. Power Sources, vol. 163, no. 1 SPEC. ISS., pp. 151–157, 2006, doi: 10.1016/j.jpowsour.2006.03.012.
[15] J. Yi, U. S. Kim, C. B. Shin, T. Han, and S. Park, “Modeling the temperature dependence of the discharge behavior of a lithium-ion battery in low environmental temperature,” J. Power Sources, vol. 244, pp. 143–148, 2013, doi: 10.1016/j.jpowsour.2013.02.085.
[16] M. Chen and G. A. Rincon-Mora, "Accurate electrical battery model capable of predicting runtime and I-V performance," in IEEE Transactions on Energy Conversion, vol. 21, no. 2, pp. 504-511, June 2006, doi: 10.1109/TEC.2006.874229.
[17] X. Zhang, “Thermal analysis of a cylindrical lithium-ion battery,” Electrochim. Acta, vol. 56, no. 3, pp. 1246–1255, 2011, doi: 10.1016/j.electacta.2010.10.054.
[18] M. Xiao and S. Y. Choe, “Theoretical and experimental analysis of heat generations of a pouch type LiMn2O4/carbon high power Li-polymer battery,” J. Power Sources, vol. 241, pp. 46–55, 2013, doi: 10.1016/j.jpowsour.2013.04.062.
[19] S. Ma et al., “Temperature effect and thermal impact in lithium-ion batteries: A review,” Prog. Nat. Sci. Mater. Int., vol. 28, no. 6, pp. 653–666, 2018, doi: 10.1016/j.pnsc.2018.11.002.